Quantum Nanospheres™
for sub-Micron Particle Image Velocimetry

Patrick Freudenthal *, Matt Pommer** & Carl D. Meinhart**

Nanex LLC, Santa Barbara, CA, USA 93109.

**Department of Mechanical & Environmental Engineering*
University of California, Santa Barbara, CA 93106

20050804 007

REPORT DOCUMENTATION PAGE

Public reporting burden for this collection of information is estimated to average 1 hour per response, including the time for reviewing instruct data needed, and completing and reviewing this collection of information. Send comments regarding this burden estimate or any other aspec. this burden to Department of Defense, Washington Headquarters Services, Directorate for Information Operations and Reports (0704-0188), 1215 Jefferson Davis Highway, Suite 1204, Arlington, VA 22202-4302. Respondents should be aware that notwithstanding any other provision of law, no person shall be subject to any penalty for failing to comply with a collection of information if it does not display a currently valid OMB control number. **PLEASE DO NOT RETURN YOUR FORM TO THE ABOVE ADDRESS.**

1. REPORT DATE (DD-MM-YYYY)	2. REPORT TYPE		3. DATES COVERED (From - To)
30-06-2005	Final		1 Sept 04 – 30 May 05

4. TITLE AND SUBTITLE	5a. CONTRACT NUMBER
Quantum Nanospheres™ for sub-Micron Particle Image Velocimetry	FA9550-04-C-0114
	5b. GRANT NUMBER
	AF04-TO24
(Nanoscale PIV)	**5c. PROGRAM ELEMENT NUMBER**

6. AUTHOR(S)	5d. PROJECT NUMBER
, UCSB	
Meinhart, Carl D, Associate Professor, Dept. of Mechanical & Environmental Engineering	**5e. TASK NUMBER**
University of California Santa Barbara, 93106	
Freudenthal, Patrick E. President, Nanex LLC	**5f. WORK UNIT NUMBER**
Santa Barbara, CA 93109	

7. PERFORMING ORGANIZATION NAME(S) AND ADDRESS(ES)		8. PERFORMING ORGANIZATION REPORT NUMBER
Nanex LLC 832 Dolores Dr. Santa Barbara, CA 03109	UCSB Santa Barbara, CA 93106	FA9550-04-C-0114

9. SPONSORING / MONITORING AGENCY NAME(S) AND ADDRESS(ES)	10. SPONSOR/MONITOR'S ACRONYM(S)
Air Force Office of Strategic Research	AFOSR
4015 Wilson Blvd, Room 743	**11. SPONSOR/MONITOR'S REPORT NUMBER(S)**
Arlington, VA 22203-1954	

12. DISTRIBUTION / AVAILABILITY STATEMENT
Approved for public release, distribution unlimited.

13. SUPPLEMENTARY NOTES

14. ABSTRACT

Quantum Nanospheres™ (QNs) have been developed as a new type of flow-tracing particle for micron resolution Particle Image Velocimetry (micro-PIV). A 60 nm diameter QN is formed by conjugating approximately eighty 10 nm quantum dots (QDs) to an individual 43 ±3 nm polystyrene bead. Since QDs have a relatively high quantum efficiency, the QNs are significantly brighter than commercially-available fluorescently-dyed particles of similar size. In addition, the 60 nm dia. QNs allow accurate velocity measurements close to microchannel walls and high spatial resolution for micro-PIV measurements. QNs maintain their fluorescent properties whether suspended in liquid or gas and may prove well-suited for gas-phase PIV.

The use of QNs as flow-tracing particles for micro-PIV was demonstrated by measuring fluid motion in a 30 x 300 μm channel. Using an interrogation region of 1 × 1024 pixels and ensemble averaging 1800 image pairs, we achieved a spatial resolution of 117 nm × 11.7 μm × 2 μm. Using 50% overlap between interrogation regions, the velocity vector spacing is ~58.6 nm. Since the QNs have a nominal diameter of ~60 nm, the particle diameter is ~50% of the smallest dimension of the interrogation region. To the best of the authors' knowledge, these velocity measurements are the highest spatial resolution measurements (based on interrogation region volume) reported to date.

15. SUBJECT TERMS
Quantum Nanosphere™, micro-PIV, quantum dots, particle image velocimetry, microfluidics

16. SECURITY CLASSIFICATION OF:			17. LIMITATION OF ABSTRACT	18. NUMBER OF PAGES	19a. NAME OF RESPONSIBLE PERSON
a. REPORT Unclassified	**b. ABSTRACT** Unclassified	**c. THIS PAGE** Unclassified	UL	14	Patrick Freudenthal
					19b. TELEPHONE NUMBER (include area code) (805) 895-9726

Standard Form 298 (Rev. 8-98)
Prescribed by ANSI Std. Z39.18

7-29-05

REPORT DOCUMENTATION PAGE (SF298) (Continuation Sheet)

1. List of Publications
(a) Manuscripts Submitted
C. D. Meinhart, P. E. Freudenthal, "Quantum Nanospheres for sub-Micron Particle Image Velocimetry", submitted to *Measurement Science Technology*, 2005
(b) Peer-reviewed Publications
(c) Non-peer-reviewed Publications
(d) Presentations

2. Demographic Data for Reporting Period
(a) Number of Manuscripts Submitted - 1
(b) Peer-reviewed Publications - 0
(c) Non-peer-reviewed Publications - 0
(d) Presentations – 1

2a. Demographic Data for life of this agreement
(a) Number of Scientists Supported by this agreement - 4
       Carl Meinhart, Ph.D., Associate Professor, MEE, UCSB
       Marin Sigurdson, Research Engineer, MEE, UCSB
       Matt Pommer, Graduate Student, MEE, UCSB
       Patrick Freudenthal, President, Nanex LLC
(b) Number of Inventions – 1
(c) Number of PhDs awarded – 0
(d) Number of Bachelor Degrees awarded as a results – 0
(e) Number of Patents Submitted – 1
(f) Number of Patents Awarded – 0
(g) Number of Graduate Students Supported – 2
(h) Number of FTE Grad Students supported – 0
(i) Number of Post Doctorate Students supported – 0
(j) Number of FTE Post Doctorate students supported – 0
(k) Number of Faculty supported by this agreement – 0
(l) Number of other staff supported by this agreement – 0
(m) Number of Undergrads supported – 0
(n) Number of Master Degrees awarded – 0

3. Report of Inventions
"Quantum Nanospheres for sub-Micron Particle Image Velocimetry," P. E. Freudenthal, C. D. Meinhart, Invention
Disclosure submitted to UC Office of Technology.

4. Scientific Progress
1. Show QDs are suitable as seed particles	completed
2. Show effective coupling of diode laser light into waveguide	completed
3. Demonstrate the feasibility of PIV with sub-micron resolution	completed
4. Explore non-traditional uses of micro / nanoPIV	completed
5. Present results at conferences	completed
6. Publish results in leading journals	completed*

          *manuscript submitted to Measurement Science Technology

5. Technology Transfer
We have submitted an invention disclosure to the university (UCSB) and expect to file a patent on a method and device. TSI has shown interest in marketing the Quantum Nanospheres™ and any nanoscale PIV instrument that may result from this contract. TSI has previously bought patents rights and subsequently marketed and is marketing instruments based on the PIV research of C. Meinhart.

1. INTRODUCTION

1.1 Micro-PIV Background

Particle Image Velocimetry (PIV) is a well-established technique for measuring velocity fields in macroscopic fluid systems.[1] Since its inception in 1997, micro-PIV has been used to measure fluid motion in microchannels, electrokinetic pumps, micro capillary electrophoretic devices, inkjets, etc. The out-of-plane resolution of micro-PIV is limited to ~2 μm, determined by the depth of field of the objective lens of the imaging system. Although nano-PIV may use similar recording optics, the depth of the evanescent field is the most significant factor determining the thickness of the interrogation region[2]. Evanescent illumination can be limited to a region with an out-of-plane dimension of ~200 nm.[3]   In the Rayleigh regime, it is difficult to image discrete particles using elastic scattering techniques. However, inelastic scattering techniques, such as fluorescence, can be used to image sub-micron particles and immobilized nano-particles.[8, 4]

The first successful micron resolution PIV experiment was reported in 1998 by Santiago et al.[5] That experimental setup is well-suited for situations where micron resolution and low-light levels are required, such as investigating flows around living microorganisms, sensitive macromolecules, or living cells. The minimum exposure time of the CCD camera required to record particle images is on the order of several milliseconds, and the time delay between image exposures is on the order of tens of milliseconds. The required exposure time and interval between exposures limits this PIV system to relatively low velocities.
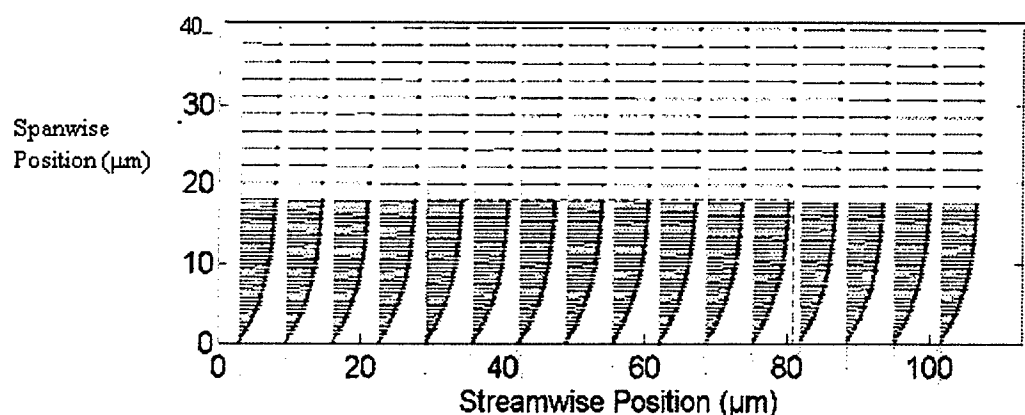

Figure 1. *Micron-resolution particle image velocimetry measurement of flow through a 30 x 300 μm channel. The resolution of the velocity vectors is 13.8 x 0.9 x 1.8 μm in the streamwise, wall-normal, and spanwise directions, respectively. The velocity vectors approach zero near the wall, suggesting that the no-slip boundary condition is accurate for hydrophilic surfaces.[6]*

In order to establish the accuracy of the micro-PIV technique, the velocity field shown in Fig. 1 was averaged in the streamwise direction to obtain an average velocity profile. This result was compared to the known analytical solution for velocity in a rectangular channel, and shown in Fig. 2. Here, the solid line is the analytical solution, and the symbols are the experimental micro-PIV data. The data agree with the analytical solution within about 2%. Therefore, we have confidence that the measurements are accurate. Figure 4 shows the velocity profile inside the microchannel for hydrophilic and hydrophobic boundary conditions. The results indicate that when the microchannel surface is hydrophobic, a slip boundary condition is present.[6]
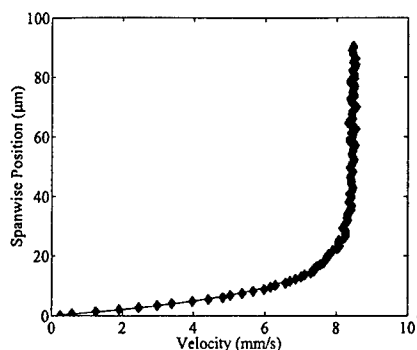
Figure 2. Ensemble-averaged velocity profile measured in a nominally 30 μm x 300 μm channel. The symbols represent streamwise-averaged PIV data, and the line is the analytical solution for Newtonian flow through a rectangular channel.[7]
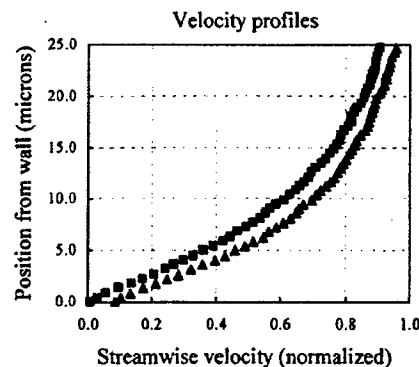
Figure 3. Velocity profiles for flow over hydrophilic (square) and hydrophobic (triangle) microchannel surfaces. The velocity profiles are normalized to the free-stream velocity.[6]

1.2 Evanescent Wave Illumination

The in-plane spatial resolution limit of micro-PIV is typically of order one micron, with an overlapping vector spacing of ~450 nm.[8] In the landmark paper by Zettner, et al. an evanescent field was used to illuminate a ~200 nm region near a microchannel wall.[2] This increased the maximum spatial resolution in the out-of-plane direction by nearly an order of magnitude while decreasing the in-plane spatial resolution by an order of magnitude. Even though the out of plane dimension is typically on the order of 100's of nanometers, the in-plane area of the interrogation region is typically on the order 10's to 100's of microns. Therefore, the averaging volume required to obtain a valid velocity measurement using evanescent illumination is similar to or larger than the averaging volume reported in volume-illuminate micro-PIV literature.[8] Even though the measurement volumes of evanescent illumination are similar to or larger than volume-illuminate micro-PIV, the evanescent illumination technique is denoted in the literature as nano-PIV. In order to minimize confusion and maintain consistency, we refer to all PIV techniques with spatial resolutions of 1 micron or less as micro-PIV.

1.3 Quantum Dots as Flow-Tracing Particles

Details of QD's – Physical Mechanism

Nanocrystals with remarkable optical properties were developed by two different research groups in the early 1980's.[9], [10], [11] These groups were able to create nanocrystal semiconductor materials capable of fluorescing at distinct visible wavelengths, depending upon the particle size. Their research laid the foundation for understanding the quantum confinement effect.[12] This effect occurs when a material/particle is of a dimension smaller than the Bohr radius of the electron-hole pair it harbors. The energy required to confine the hole-pair is apparently the source of the large band gap.[13]

The quantum dots used in these experiments have a core of cadmium selenide (CdSe) An inorganic passivating coating of zinc sulfide (ZnS) adds to their solubility in water.[14] An additional polymer shell allows bio-conjugation to a variety of molecules, such as biotin.

Because QDs are ~10 nm in diameter, they exhibit significant Brownian motion, which can create significant noise in the velocity signal. Pouyal et al. recently demonstrated that individual QDs could be used as flow-tracing particles with evanescent illumination. As expected, the error due to Brownian motion was approximately 57% full scale.[15]

1.4 Error due to Brownian Motion

Errors resulting from Brownian motion strongly depend upon the characteristic velocity of the fluid and the size of the flow-tracing particle. As the spatial resolution of PIV systems approach the ~100 nanometer range, the size of the flow-tracing particles must decrease to the 10 – 100 nm diameter range. The small particle size can create significant stochastic noise in the underlying velocity signal, due to Brownian motion. Therefore, in order to achieve nanometer resolution PIV, it is important to develop seed particles small enough to achieve the desired spatial resolution and follow the flow faithfully, yet large enough to dampen Brownian motion and be visible. (See Fig. 4)

The Stokes-Einstein equation can be used to estimate the diffusion coefficient for a spherical particle in a Newtonian fluid

$$D = \frac{k_B T}{3\pi \mu d_p},$$

(1)

where D is the Brownian diffusion coefficient, k_B is Boltzmann's constant, and T is the absolute fluid temperature, μ is the dynamic viscosity of the working fluid, and d_p is the seed particle diameter. Santiago et al.[5] gave a first order estimate of the error due to Brownian motion relative to the displacement in the x-direction, ε_B.

$$\varepsilon_B = \frac{\langle s^2 \rangle^{1/2}}{\Delta x} = \frac{1}{u}\sqrt{\frac{2D}{\Delta t}},$$

(2)

where s^2 is the random mean square particle displacement associated with Brownian motion, Δx is the characteristic particle displacement, u is the characteristic velocity of the fluid, and Δt is the time interval between images. Equations (1) & (2) show the inverse relation of diffusion to particle size and the viscosity of the fluid.
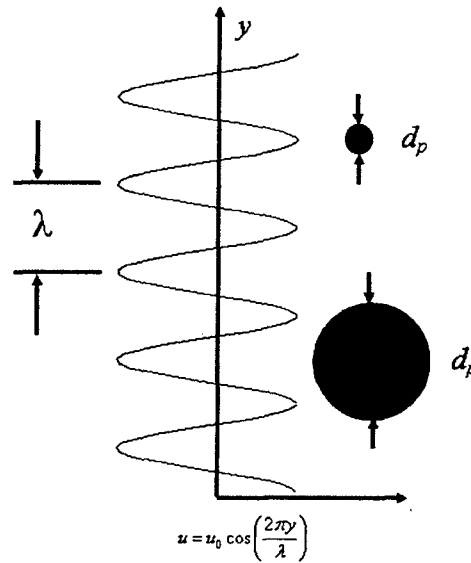

Figure 4. Illustration showing the effect of particle size on spatial resolution. Larger particles cannot adequately resolve fluid motion. With quantum dot-sized particles random (Brownian) motion will cause smearing of the measured velocity field.

In practice, the error due to Brownian motion places a lower limit on particle size. The Brownian error is lower for high velocity flows. For given flow conditions, increasing the time delay between successive images, Δt, can also reduce the Brownian error. However, the range of time delay is limited by the desired spatial resolution and the field of view of the imaging system.

2. QUANTUM NANOSPHERE™ DEVELOPMENT

2.1 Motivation for Quantum Nanospheres™ QNs

There are many factors that limit spatial resolution of micro-PIV systems.[1] One of these factors is, of course, the size of the flow-tracing particle. In all PIV instruments, the underlying spatial resolution cannot be smaller than the physical size of the flow-tracing particles. For spatial resolutions approaching order 100 nm, the flow-tracing particles must be less than ~100 nm in diameter. Fluorescently-dyed particles 100 nm or larger can be imaged readily by epi-fluorescent microscopes.[8] However, fluorescently-dyed particles smaller than ~100 nm are not easily imaged because the fluorescent dye is not sufficiently bright. High intensity illumination tends to photobleach the fluorophores and therefore degrades the fluorescent particle images. Fluorophores typically have a narrow Stokes shift (~50 nm) that results in a low signal-to-noise ratio. Quantum dots, however, have distinct advantages compared to particles that use fluorescent dyes: (1) the quantum efficiency of the QDs is significantly higher than fluorophores, (2) they do not photo-bleach, (3) they have a significant Stokes shift (~250 nm)[1617], (4) they have a narrow emission spectra, and (5) they maintain their fluorescent properties when suspended in a gas, making them well-suited for gas-phase micro-PIV.

Initially, individual ~10 nm diameter quantum dots (QDs) were considered as seed particles as an alternative to fluorophores. QDs are easily imaged with standard micro-PIV instrumentation when they are immobilized on a glass slide. However, there are three main reasons individual QDs do not make suitable seed particles for micro-PIV. 1) exposure times required to image them is on the order of milliseconds, which would prevent PIV measurements in high-speed streams. 2) their small size makes them highly susceptible to Brownian motion, creating noise in the velocity signal. 3) individual QDs blink on and off intermittently due to quantum effects, thereby contributing to seed particle dropout and reducing the velocity signal.

Quantum Nanospheres™ (QNs) were developed to address the drawbacks of using individual QDs as PIV seed particles. QNs are created by attaching a number of QDs to polystyrene beads (see Figs. 5 & 6). QDs emit a strong fluorescent signal with a wide Stoke's shift, in the range of 100s of nanometers. The combined output of eighty QDs bound to a single polystyrene bead is sufficient to be imaged by a sensitive CCD camera. In addition, a 60 nm dia. QN has six times less Brownian motion than an individual 10 nm dia. QD and provides less noise in the resulting velocity measurements. In addition, the QD blinking problem is eliminated by conjugation of tens of QDs onto a single polystyrene bead.

2.2 Synthesizing Quantum Nanospheres™

We synthesized QNs by conjugating 10 nm dia. biotinylated QDs (Item 80-0204, Quantum Dot Corp., Hayward, CA) to 43±3 nm dia. polystyrene beads (PSBs) activated with streptavidin (Bangs Laboratories, Fishers, IN). The solution containing the beads was titrated into the QD solution over the space of ~1 minute, while stirring. Immediately after 15 μl of free biotin solution was added to quench the reactions by filling any remaining streptavidin binding sites. Figure 5 shows a depiction of the QN conjugation chemistry. The QDs efficiently absorb UV/blue light at λ ~300-450 nm, and emit red light at λ ~ 655 nm. The emission and absorption spectra for these QDs are shown in Fig. 7. Non-fluorescing 43±3nm diameter PS beads coated with *NeutrAvidin™* were chosen so that the resulting QNs would be approximately 60 nm in diameter. This size is confirmed by SEM images of the QNs (see Fig. 6). These particles are small enough to allow for high spatial resolution and large enough to sufficiently dampen Brownian motion while capable of being imaged with a non-intensified CCD camera.
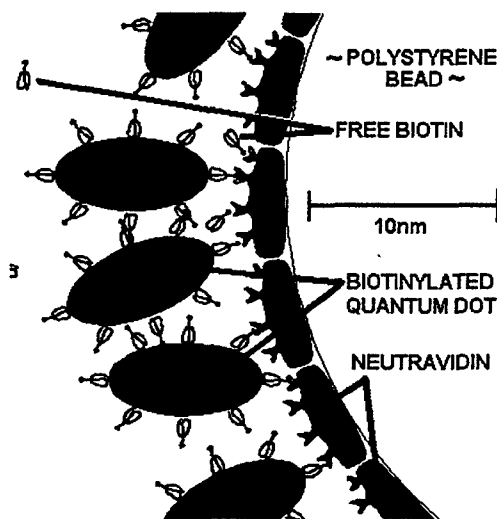
Figure 5. Beads coated with NeutrAvidin™ were titrated into a solution containing biotinylated quantum dots. Free biotin was added after the beads were coated with QDs so remaining NeutrAvidin™ binding sites would be filled.
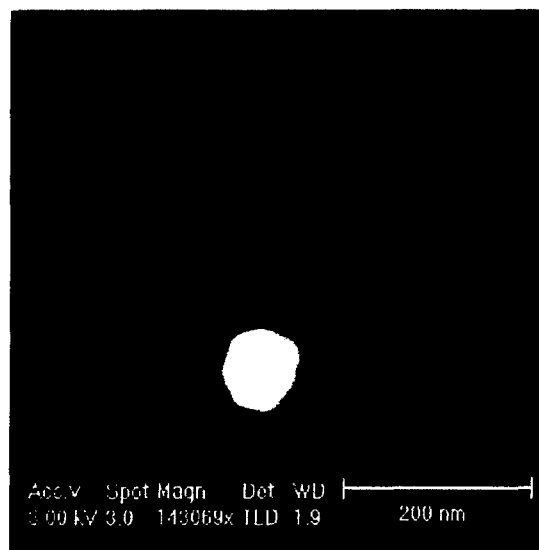
Figure 6. Scanning electron microscope (SEM) image of a Quantum Nanosphere™ - colorized for contrast. A ~3 nm layer of gold was deposited over the QN to carry away electrons from the SEM probe. Estimated diameter of the QD is 65 nm

The concentrations and volumes were selected [what were they – how much of what?] to provide an excess of QDs. This ensured complete and rapid coating of the PS beads with QDs. Care was taken to ensure that a significant portion of QNs did not conjugate to each other, which would create clumps of QNs.. Samples of the resulting QN solution were dried on slides and examined for particle size and consistency. The inset in Fig. 8 is an optical image of QNs, depicting two single QNs and a co-joined QN with twice the intensity of the single QN.

The SEM image in Fig. 9 shows bright QNs and significantly less bright QDs. The QNs have good contract when compared to the background and are are uniform in size.

There is room for approximately eighty 10 nm dia. QDs on an individual 43 nm PSB, assuming the QDs are geometrically close-packed. The QDs and PSBs are mixed in a solution with approximately 240 QDs for each PSB. The factor of three-fold oversupply of QDs was chosen to ensure that all the PSBs become fully coated with QDs and the resulting QNs have maximum brightness and uniform properties.

The PSBs were successfully coated with QDs producing QNs, with only about 0.1% of them appearing to be multi-bead clusters. Optically imaged at 60x the vast majority of the particles in solution appeared to be individual QNs of moderately uniform brightness. Multi-bead clusters appeared brighter than single beads and as they randomly rotate about their center of gravity they are readily distinguishable from single-bead QNs (see Fig. 8).

The solution used for PIV contained both QDs and QNs. A greater signal-to-noise ratio could be achieved by separating the free QDs from the solution. When the solution is left stagnant for several hours, the QNs tend to cluster. Therefore, the QN solution is sonicated before each use. Figure 8 is an image of QNs in a solution that was not sonicated. Fig. 9 shows that same solution after it was dried on a glass slide.
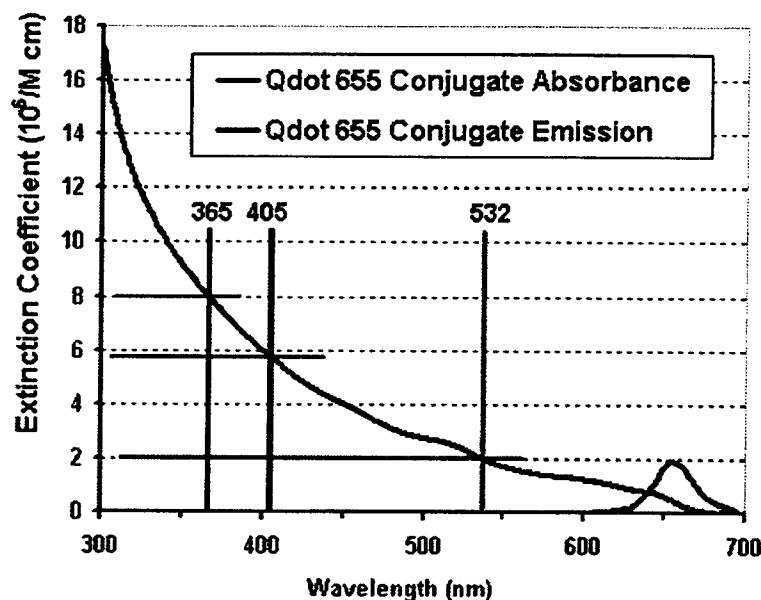
Figure 7. *Extinction/emission plot of Qdot conjugate and details at specific wavelengths. The 405 nm excitation used in this experiment contrasts well with the excitation expected from an Nd:YAG laser frequency-doubled to 532 nm.*

In optical images, the QDs and QNs are diffraction limited.[18] Their effective particle image diameter was approximately the diameter of the point spread function of the microscope recording optics. As illustrated in the inset in Fig. 5, the image diameter of a 60 nm QN is imaged over 3 pixels. When projected back into the flow, the effective image diameter was approximately 300 – 400 nm.
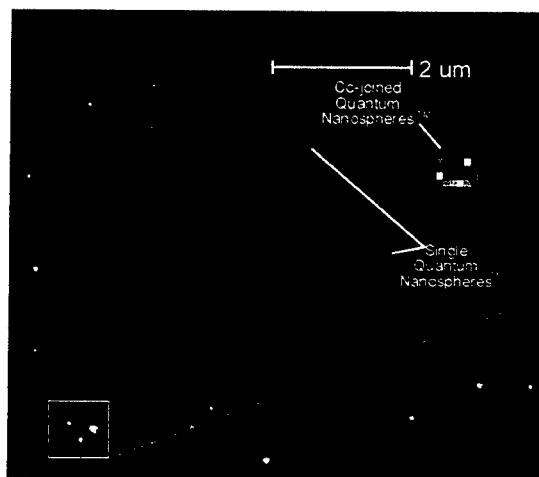
Figure 8. *Opitcal images of Quantum Nanospheres[TM] (QNs) and quantum dots (QDs) in solution. Particle brightness is affected by particle size and position relative to the image plane of the microscope. Large variation in brightness shown indicates co-joined QNs.*
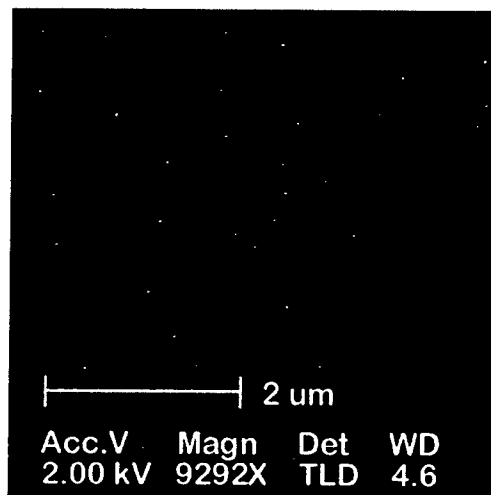
Figure 9. *SEM image of QNs and QDs immobilized on a glass slide. The brighter dots are QNs that appear to be uniform in size and distribution. Viewed optically, QDs exhibit scintillation, while QNs overcome this drawback by incorporating multiple QDs.*

2.3 Quantum Nanospheres as Seed Particles - Microchannel Flow Experiments

In order to demonstrate the utility of QNs as PIV seed particles for ~ 100 nm spatial resolution, micro-PIV measurements were obtained in a 30 x 300 microchannel (Wilmad LabGlass, Buena, New Jersey). The microchannel was mounted on a glass slide and epoxied to tygon tubing (see Figs. 10 & 11). The micro-PIV measurements were conducted using an inverted fluorescent microscope system (Nikon® Eclipse TE200, Tokyo, Japan). A schematic of the experimental apparatus is shown in Fig. 12.
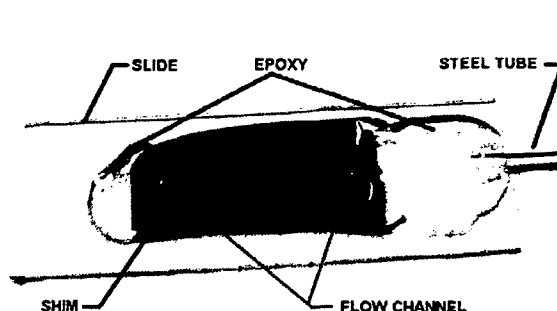

Figure 10. A glass flow channel mounted on a standard microscope slide using epoxy. A shim (black) adjusts the height of the channel to minimize bending when attaching tubing.
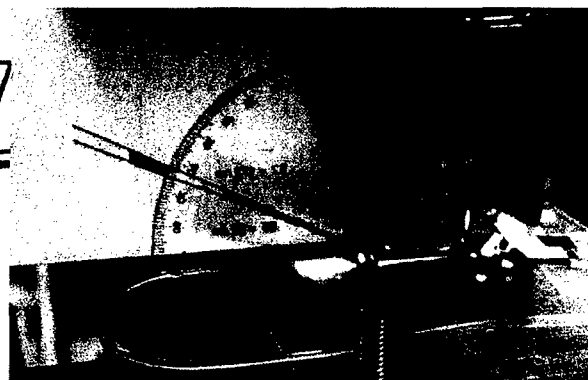
Figure 11. Waveguide with Tygon tubing attached is illuminated by an evanescent field. An air gap was required between the lens and waveguide, as an oil immersion lens interfered with the evanescent field.

A 35 mW λ = 405 nm CW diode laser (Sanyo #5146-351, Photonic Products, Huntington Beach, CA) was operated in pulse mode. A δt = 4 ms duration light pulse from the diode laser was directed onto the microchannel to illuminate the QNs. Fluorescent light from the QNs was collected by an M = 60, NA = 1.4 oil-immersion lens. The filter cube consisted of a 475 nm long-pass dichroic filter (475DCXRU, Chroma Corp, Rockingham, VT) and a bandpass emission filter with a center wavelength of 655 nm and half-power bandwidth of 20 nm (XF2203 and XF3305, Omega Optical, Brattleboro, VT), Due to the large Stokes shift of the seed particles no excitation filter was required.

The particle-image fields were captured by an interline transfer 1376 × 1024 pixel × 12 bit resolution CCD camera (Model 630047, TSI, Inc., St. Paul, MN) capable of taking two images within a time interval as short as 200 ns.. The image recording process was repeated to capture the particle images after a Δt = 40 ms time delay.

The working fluid was DI water with a dilute suspension of QNs at a volume fraction of 0.00084%. 1800 pairs of image fields were recorded during each experimental run. The high number of image field pairs compensates for the low seeding density of the QNs and provides sufficient signal to obtain high spatial resolution. A flow rate of 4.5 nl/s was generated using a gravity-feed system with a reservoir positioned 45 cm above the microchannel.
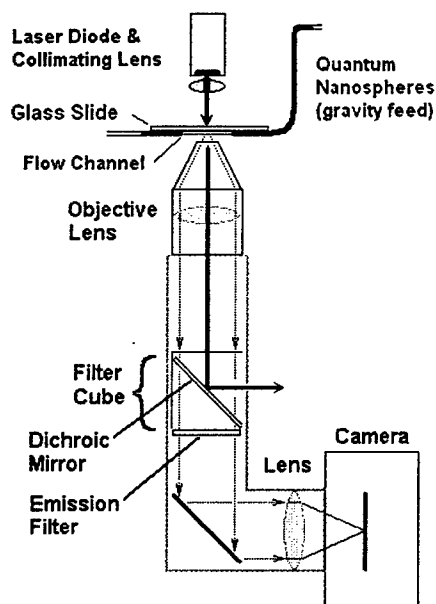
Figure 12. *The optical setup: Nikon TE200 inverted microscope with 60X oil-immersion lens, TSI CCD camera, and 35 mW, 405 nm laser diode with collimating lens for illumination.*

3. VELOCIMETRY RESULTS

3.1 Interrogation Analysis

Analysis was carried out using ensemble averaging of the image pairs. The average background was calculated and subtracted from each image before analysis. The background averaging, subtraction and subsequent ensemble averaging was carried out using MatLab software (The MathWorks, Inc., Natick, MA) and proprietary MatLab scripts.

An interrogation window size of 1024x6 pixels was selected. Correlation over 1024 pixels in the X (streamwise) direction maximized the signal-to-noise ratio of the resulting U (streamwise) velocity vector field. Correlation over 6 pixels in the Y (wall-normal) direction maximized the resolution between vectors. By overlapping the interrogation cells by 50%, velocity vectors were obtained at every 58.6 nm in the wall normal direction.

The minimum limit of the analysis software was brought to a single pixel in the wall normal (Y) direction by digital enlargement of the data set in the Y direction only. Image sets magnified 300% and 600% were processed and compared to the unenlarged data set.

3.2 Details of the Fluid Motion

The velocity vectors very near the wall (<1 micron) were considered unreliable and are not shown in the figures below. The seed particles could be observed to move in erratic patterns near the wall as Brownian motion and other factors caused them to move toward the wall, slow or stop, then resume moving with the stream. The error in the smoothed

The resolution of the unenlarged image has been improved sixfold through digital magnification and subsequent analysis. Each of the graphs on the left (Figs. 13, 15, & 17) are from raw data. The graphs on the right (Figs. 14, 16, & 18) show the same data after interpolation of missing vectors and smoothing using a 3x3 Gausian kernel. Error in the raw data is <10%.
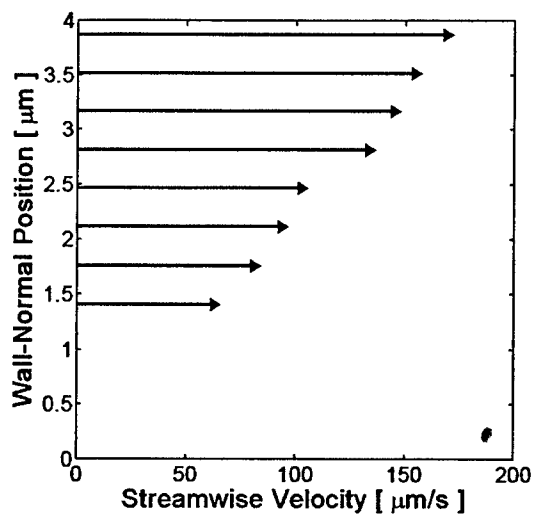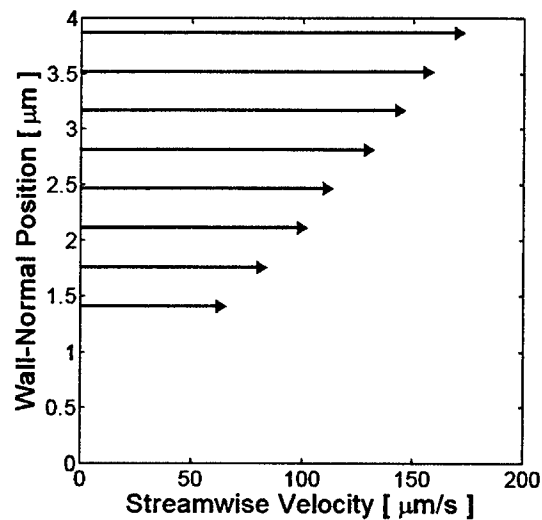
Figure 13. *1024x6 pixel unsmoothed*
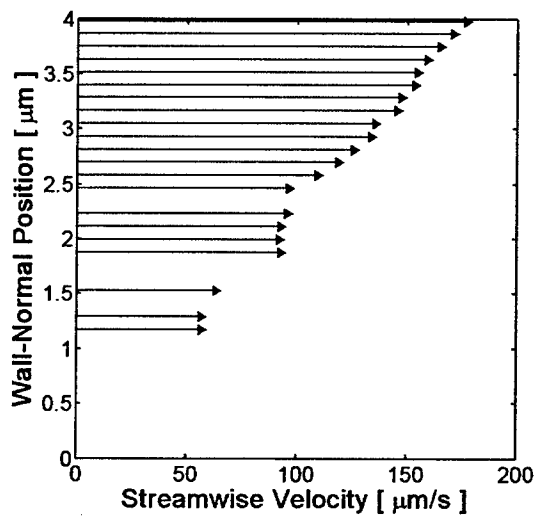

Figure 14. *1024x 6 pixel smoothed*

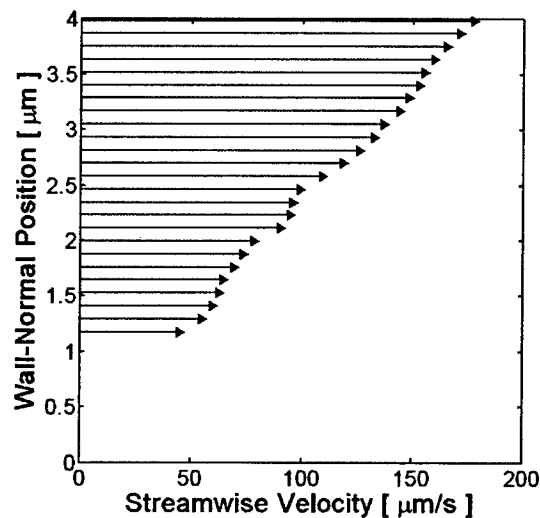**Figure 15.** *1024x 3 pixel unsmoothed*

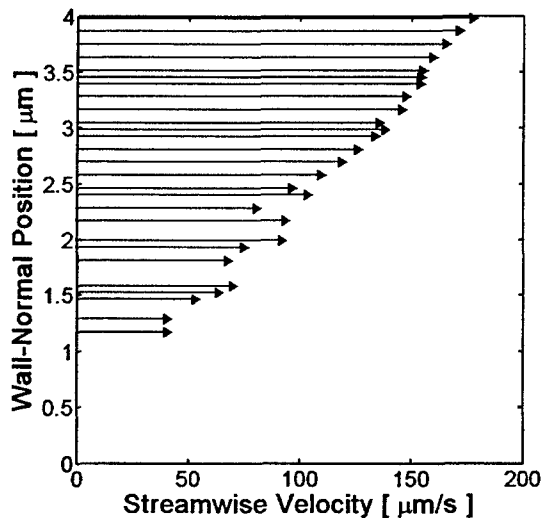**Figure 16.** *1024x 3 pixel smoothed*
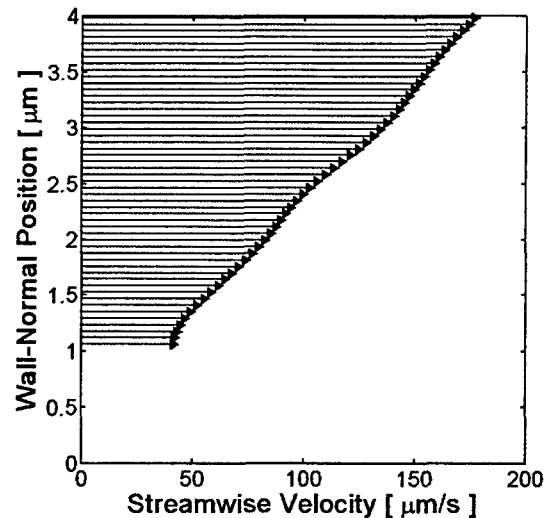
Figure 17. *1024x 1 pixel unsmoothed*

Figure 18. *1024x 1 pixel smoothed*

4. DISCUSSION

High spatial resolution was achieved in flows up to 500 μm/s by using a 4 ms pulse from a diode laser operating at λ= 407 nm to illuminate sub-micron fluorescent particles. The experiments conducted were solely to prove the feasibility of high velocity, high resolution PIV. Experimental elements were not optimized and in many cases were quite rough. However, the results indicate that with the use of QNs of appropriate size allows high spatial resolution by minimizing Brownian motion without impeding the seed particles ability to accurate follow the fluid flow.

4.1 Potential spatial and temporal resolution

The potential spatial and temporal resolution are limited by the power of the laser, the sensitivity of the CCD, the optics and the characteristics of the seed particles. Spatial resolution can be improved by using optical components with a higher resolution. A higher sensitivity CCD, or running the CCD at lower a temperature would both be of benefit.

There may be tradeoffs in making changes to the system. Employing a higher magnification objective (100x rather than 60x) may improve spatial resolution but will reduce the light falling on each pixel of the CCD. Measuring high-velocity (~1000 m/s) flows will require not only lasers and timing schemes capable of nanosecond-scale illumination pulses, but will also require those lasers to deliver high energy in that short time – on the order of tens to hundreds of Watts. The optical components (lenses, filters, etc.) must be capable of withstanding such power.

4.2 Potential Dynamic Range using Quantum Nanospheres™

To investigate the feasibility of making useful measurements – those with an error <10% of the signal – we plotted the range over which a 50 nm diameter QD could be successfully imaged (Fig 19).

The dynamic range may be improved by increasing the number of seed particles in each image and by increasing the number of image pairs. Either method has its difficulties.

Greater particle density in the image field also means greater background noise. The particle density was adjusted but not optimized for particle density vs. signal-to-noise ratio.

Increasing the number of images increases the overall length of the experiment. To capture 3600 images required ~40 minutes. Changes over time in illumination intensity may occur due to heating, power fluctuation, etc. Flow variations may occur due to blockage of the flow path, etc. It may be possible to correct for background variations over time by subtracting background noise of groups of adjacent images rather than subtracting the average of all images. However, there is a limit to how many images may be captured while maintaining a stable system.

For statistically independent events the uncertainty in particle displacement decreases $\sim 1/\sqrt{N}$, where N is the number of particles contained in the sample average. Using a sample of 10 particles and averaging over 100 image intervals, the velocity dynamic range in nanochannels can be increased by a factor of $\sim \sqrt{1000} = 33$. In practice we averaged over 1800 intervals for a calculated improvement in resolution by a factor of 42 – ignoring any variations in system parameters noted in the paragraph above.
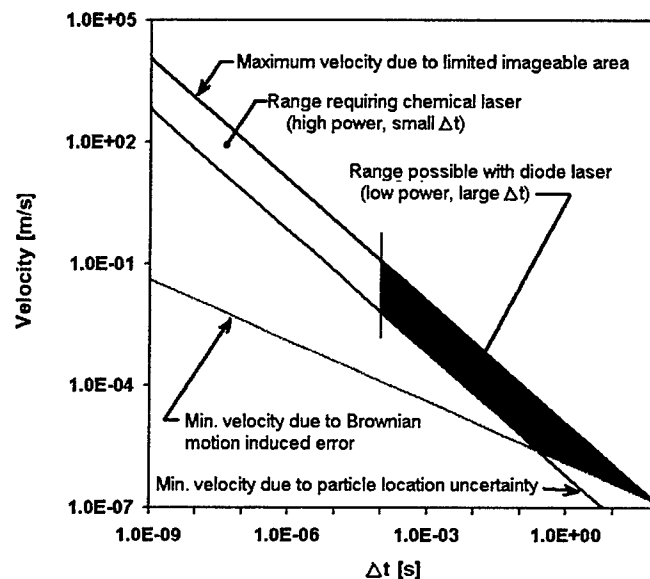

Figure 19. *Instrument Dynamic Range (Velocity) for a 50 nm diameter particle given ε_B = 10%, and averaging over 10 particles and 100 image intervals. The graph show maximum and minimum measurable velocities as function of time delay, Δt.. In practice we greatly improved dynamic range by ensemble averaging over 1800 image pairs.*

Assuming the particle image is sufficiently resolved by the CCD array, requiring ~3-4 pixels per image diameter, the location of a particle can be estimated to within ~1/10th the diameter of its diffraction-limited image.[5],[19] For a 640 nm image the uncertainty of its location is

$$\delta x \approx \frac{640 \text{ nm}}{10} = 64 \text{ nm} . \tag{3}$$

The error due to uncertainly in particle image location relative to the displacement Δx is given by

$$\varepsilon_{\delta x} = \frac{\delta x}{\Delta x} . \tag{4}$$

If we set $\varepsilon_{\delta x} = 0.10$ and $\delta x = 64$ nm , we can determine the minimum distance a particle must travel to obtain an accurate measurement, $\Delta x_{min} = 0.64 \mu m$. This places a limit on the minimum velocity

that may be accurately measured for a given time delay. Given this minimum value of Δx, we can calculate a minimum velocity required for a given Δt.

The maximum measurable velocity is determined by the specified minimum time delay between images and either the desired in-plane spatial resolution or the field of view of the imaging system, x_{FoV}, such that

$$u_{max} = \frac{x_{FoV}}{\Delta t} .$$

(5)

In a PIV system with a nominal CCD resolution of 1024 pixels in the x direction, 6.8 μm pixel spacing, and an M=60x magnification, the field of view is typically x_{FoV} ~ 100 μm. This sets the maximum velocity dynamic range to approximately 70:1. However, if one is measuring flow through a 100 nm channel for example, particle displacements of more than 70 channel widths (~7 μm) are unacceptable. A practical limit for the dynamic range for measurement in nanochannels is ~ 10:1.

4.3 Application to Gas-Phase PIV

High-speed gas flow through micronozzles can exhibit accelerations of order 70 million g's. Assuming Stokes' drag, small flow tracing particles of order 50-100 nm are required to adequately follow the flow.[20] Meinhart el al. demonstrated that reflective Differential Interference Contrast (DIC) microscopic techniques could be used to image 50 nm glass particles in air. Unfortunately, DIC can only be used with incoherent light sources. Laser speckle tends to drown out the particle images, thereby limiting the utility of DIC for high-speed micro-PIV applications. However, the fluorescent properties of QNs may be an ideal flow-tracing particle for gas-phase micro-PIV, and well-suited for laser illumination in gas flows.

Meinhart et al. showed that clumping of particles due to electrostatic forces was a significant problem in gas-phase PIV. A device is now commercially-available (Model 3480 Electrospray Aerosol Generator , TSI, St. Paul, MN) that is capable of dispersing nanometer-scale particles in a range of <3 to >100 nm in a neutralized, monodisperse aerosol, with little solvent residue.[21] The use of QNs as seed particles may allow high resolution fluorescence-based PIV in high-velocity gases that is not possible with dye-based particles or DIC techniques. High temporal resolution PIV will require a mode-locked YAG laser, Titanium-Sapphire (Ti-S) laser or other source with pulse durations ranging between 50 fs - 100 ps.

With these new technology developments, gas-phase micro-PIV is now feasible.

CONCLUSIONS

We have demonstrated that high resolution, high velocity PIV is feasible. A new type of micro-PIV particle termed a Quantum Nanosphere™ (QN) has been developed by conjugating quantum dots to polystyrene beads. The resultant particle is bright enough to be readily imaged using an non-intensified CCD camera, and a low power (35 mw) CW laser for illumination. QNs have numerous advantages over dye-based fluorophores. They exhibit significantly less Brownian motion than a quantum dot (QD). The QNs are small enough to accurately follow the flow near the wall in microchannels and nanochannels. Their size and their fluorescence when suspended in gas may prove ideal for gas-phase PIV.

Development of the Quantum Nanosphere™ enabled high resolution PIV in a flow velocity range of 0-500 μm/s using a low power (35 mW) diode laser. High-powered lasers could be used to extend the range of velocity measurements by orders of magnitude. Velocity-vector fields were measured with a spatial resolution of 117 nm x 11.7 micron x 2 micron. This gives an interrogation volume of 8 microns cube or 1.4 fL. In terms of physical interrogation volumes, this is the highest spatial resolution published to date.

REFERENCES

1 Adrian, R, 1991. Particle-imaging techniques for experimental fluid mechanics. Annu. Rev. Fluid Mech, Vol. 23:261-304.

2 Zettner, C; Yoda, M, 2003. Particle velocity field measurements in a near-wall flow using evanescent wave illumination, Experiments in Fluids, Volume 34 Number 1:115-121.

3 Jin, S., Huang, P, Park, J. and Breuer, K.S. "Near-Surface Velocimetry using Evanescent Wave Illumination". IMECE2003-44015. In Proceedings of ASME-IMECE. Washington DC, November 2003; Jin, S., Huang, P., Park, J., You, J. Y., & Breuer, K. S. "Near-wall PTV measurements using evanescent wave illumination". PIV '03 Paper 3237. Proceedings 5th International Symposium on PIV. Busan, Korea. Sep, 2003.

4 Molecular Probes, Inc., Handbook for Fluorescent Probes and Research Products, www.probes.com. 2004.

5 Santiago, J; Wereley, S; Meinhart, C; Beebe, D; Adrian, R, 1998. A micro particle image velocimetry system. Exp. Fluids, Vol. 25 No.4:316-319.

6 Tretheway, D; Meinhart, C, 2002. Apparent fluid slip at hydrophobic microchannel walls, Physics of Fluids, Volume 14, Number 3:9-12.

7 Meinhart, C; Santiago, J; Adrian, R; Wereley, S, 2003. Micron resolution particle image velocimeter. United States Patent 6,653,651.

8 Meinhart, C; Wereley, S; Santiago, J, 1999. PIV Measurements of a Micro/nanochannel Flow. Exp. in Fluids, Vol. 27:414-419.

9 Brus, L. E. Electron-Electron and Electron-Hole Interactions in Small Semiconductor Crystallites: The Size Dependence of the Lowest Excited Electronic State. J. Chem. Phys.1984, 80, 4403-4407.

10 Efros, Al. L.; Efros, A. L. Interband Absorption of Light in a Semiconductor Sphere. Sov. Phys. Semicond.1982, 16, 772-774. Ekimov, A. I.; Efros, Al. L.; Onushchenko, A. A. Quantum Size Effect in Semiconductor Microcrystals. Solid State Commun. 1985, 56, 921-924.

11 Brus, L.E., A simple model for the ionization potential, electron affinity, and aqueous redox potentials of small semiconductor crystallites. J.Chem.Phys. 79(11) 5566-5571, 1983.

12 Wilson, W. L., Szajowski, P. F., and Brus, L. E., Quantum Confinement in Size-Selected, Surface-Oxidized Silicon Nanocrystals", Science, vol. 262, 1242-1244, Nov., 1993.

13 Quantum Dot Corp. www.qdot.com.

14 Wu X.,2003. Detecting nuclear antigens using QdotTM streptavidin conjugates. Quantum Dot Vis 1:10–13.

15 Pouyal S., Koochesfahani, M., Preston Snee, P., Bawendi, M., Nocera, D. Single Quantum Dot (QD) Imaging of Fluid Flow Near Surfaces, accepted for pub. in Experiments in Fluids, May 16, 2005.

16 Ness, J.M., Akhtar, R.S., Latham, C.B., and Roth, K.A., 2003.: Combined Tyramide Signal Amplification and Quantum Dots for Sensitive and Photostable Immunofluorescence Detection, The Journal of Histochemistry & Cytochemistry, Volume 51(8): 981–987.

17 Watson A, Wu X, Bruchez M (2003) Lighting up cells with quantum dots. BioTechniques 34:296–303.

18 Meinhart, C; Wereley, S, 2003. The theory of diffraction-limited resolution in microparticle image velocimetry. Institute of Physics Publishing, Measurement Science and Technology, Vol 14:1047–1053.

19 Prasad, A.K., Adrian, R.J., Landreth, C.C., and Offutt, P.W., "Effect of Resolution on the Speed and Accuracy of Particle Image Velocimetry Interrogations," Experiments in Fluids, Vol. 13, No. 2-3, pp. 105-116, 1992.

20 C. D. Meinhart, M. H. B. Gray & S. T. Wereley, PIV Measurements of High-Speed Flows in Silicon-Micromachined Nozzles, AIAA-99-3756.

21 TSI Inc., http://www.tsi.com/documents/3480.pdf.